INSTITUTE OF PHYSICS PUBLISHING JOURNAL OF OPTICS A: PURE AND APPLIED OPTICS
J. Opt. A: Pure Appl. Opt. **7** (2005) 238–248 doi:10.1088/1464-4258/7/5/005

Force on a scatterer in counter-propagating coherent beams

John Lekner

School of Chemical and Physical Sciences, Victoria University of Wellington, PO Box 600, Wellington, New Zealand

Received 10 January 2005, accepted for publication 7 March 2005
Published 30 March 2005
Online at stacks.iop.org/JOptA/7/238

Abstract
Counter-propagating coherent beams produce fringes, with intensity proportional to $\cos^2 kz$ in the plane wave case. A scatterer placed in the fringing field experiences a force, except when centred on an intensity maximum or minimum. We show that, for displacement b from an intensity maximum, the force is $\sin 2kb$ times a *force factor*. The force factor is independent of b, and depends on the interaction of the spherical scatterer with a (unidirectional) plane wave. This result is universal for spherical scatterers, and holds in both the quantum particle and electromagnetic cases. For a given type of scatterer, the force factor depends on the ratio of scatterer size to wavelength in an oscillatory way, so for different radius/wavelength values the scatterer may be in stable equilibrium at intensity maxima or at intensity minima, or may even not feel a force at all.

Keywords: radiation forces, optical tweezers

(Some figures in this article are in colour only in the electronic version)

1. Introduction

The motivation for this study comes from the experiments of Mellor and Bain [1] on micron-sized dielectric spheres trapped in the evanescent field of coherent counter-propagating electromagnetic waves. Potential applications are manipulation of sphere arrays, creation of tunable diffraction gratings, micron-sized particle conveyor-belts, and the study of two-dimensional colloidal crystals. Earlier works with such particles in evanescent fields had the radiation propagating in one direction only [2–4]. One might think at first that there should be no force along the direction or propagation when two equal beams (evanescent or not) oppose each other. This is not so: the two beams, being coherent, produce interference fringes, and the net transfer of momentum from fields to particle is not zero in general, unless the (spherical) particle happens to be at an interference maximum or minimum. We shall show that, in both the quantum scalar case and the vector electromagnetic case, the force on a spherical particle has the form

$$f(k, s, b) = F(k, s) \sin 2kb \tag{1}$$

where $k = 2\pi/\lambda$, s denotes parameters characterizing the interaction of the beams with the scatterer (such as its radius), and b is the distance between the scatterer centre and a constructive interference maximum. The result (1) may equivalently be written as

$$f(k, s, b) = \frac{\partial U}{\partial b}, \qquad U(k, s, b) = -k^{-1} F(k, s) \cos^2 kb; \tag{2}$$

i.e. an effective potential proportional to $\cos^2 kb$ quantifies the interaction of the sphere with the coherent counter-propagating beams. (The sign in (2) is in accord with our choice of moving the fringes, and keeping the scatterer fixed at the origin.)

We shall derive expressions for the force factor in both the scalar (Schrödinger) and vector (Maxwell) cases, in sections 3 and 6, respectively. In both cases the force factor is given in terms of parameters characterizing the interaction of the scatterer with a plane wave. These are respectively the partial wave phase shifts δ_ℓ, and the Mie–Debye coefficients a_ℓ, b_ℓ. To introduce the notation and method, we begin with a calculation of the force on a scatterer in a unidirectional quantum beam.

2. Force on a scatterer in a particle beam

Let the interaction potential between the scatterer and the particles forming the beam be $V(r)$ (we assume a central

interaction, with the scatterer fixed at the origin). The Schrödinger equation for a monoenergetic beam of particles of mass m and energy $e = \hbar^2 k^2/2m$,

$$\left(\nabla^2 + k^2 - \frac{2mV}{\hbar^2}\right)\psi = 0, \tag{3}$$

is solved, outside the range of V, by

$$\psi(r,\theta) = \sum_{\ell=0}^{\infty}(2\ell+1)\mathrm{i}^\ell \mathrm{e}^{\mathrm{i}\delta_\ell}[\cos\delta_\ell j_\ell(kr) - \sin\delta_\ell n_\ell(kr)]P_\ell(\cos\theta). \tag{4}$$

(Standard notation for phase shifts δ_ℓ, spherical Bessel functions j_ℓ and n_ℓ, and Legendre polynomials P_ℓ is being used: see for example [5] (section 19).) The form of (4) is determined by the requirement that for large kr the wave should consist of the incident plane $\mathrm{e}^{\mathrm{i}kz}$ plus a spherically diverging scattered wave $r^{-1}\mathrm{e}^{\mathrm{i}kr}f(\theta)$, where $f(\theta)$ is the scattering amplitude. From (4) and the asymptotic forms of the spherical Bessel functions one finds

$$f(\theta) = k^{-1}\sum_{\ell=0}^{\infty}(2\ell+1)\mathrm{e}^{\mathrm{i}\delta_\ell}\sin\delta_\ell P_\ell(\cos\theta). \tag{5}$$

The phase shifts δ_ℓ of the partial waves are determined by solving Schrödinger's equation inside the scatterer, and matching with (4) which holds outside the scatterer. For example, an impenetrable sphere of radius a has $\psi = 0$ for $r \leqslant a$, which gives

$$\tan\delta_\ell = \frac{j_\ell(ka)}{n_\ell(ka)}. \tag{6}$$

To find the force exerted by a single beam (represented by the plane wave $\mathrm{e}^{\mathrm{i}kz}$) on a scatterer, one calculates the momentum transfer cross-section

$$\sigma = 2\pi\int_0^\pi \mathrm{d}\theta\ \sin\theta(1-\cos\theta)|f(\theta)|^2. \tag{7}$$

With the use of (we write C for $\cos\theta$)

$$\int_{-1}^{1}\mathrm{d}C\,P_\ell(C)P_{\ell'}(C) = \frac{2}{2\ell+1}\delta_{\ell',\ell}$$

$$\int_{-1}^{1}\mathrm{d}C\,C\,P_\ell(C)P_{\ell'}(C) = \frac{2(\ell+1)}{(2\ell+1)(2\ell+3)}\delta_{\ell',\ell+1} + \frac{2\ell}{(2\ell-1)(2\ell+1)}\delta_{\ell',\ell-1} \tag{8}$$

one finds [6]

$$\sigma = \frac{4\pi}{k^2}\sum_{\ell=0}^{\infty}(\ell+1)\sin^2(\delta_\ell - \delta_{\ell+1}). \tag{9}$$

The z-component of the momentum of a particle within the beam, when scattered through angle θ, changes from $\hbar k_z = \hbar k$ to $\hbar k_z' = \hbar k\cos\theta$, so it is decreased (in the forward direction) by the factor $1-\cos\theta$: hence the definition (7). The force on the scatterer due to scattering is the rate of change of momentum within the beam, namely

$$\text{force} = N\frac{\hbar k}{m}\sigma\hbar k = 2Ne\sigma \tag{10}$$

where N is the particle density (number per unit volume) in the incident beam, $\hbar k/m$ is their speed, σ is the effective scatterer area for transfer of momentum, and $\hbar k$ is the momentum per particle in the beam.

3. Force on a scatterer in counter-propagating particle beams

A plane wave $\mathrm{e}^{\mathrm{i}kz}$ incident on a spherical scatterer fixed at the origin produces a scattered wave $\psi_\mathrm{s}(r,\theta) \equiv \psi(r,\theta) - \mathrm{e}^{\mathrm{i}kz}$. From (4) and the spherical Bessel expansion of a plane wave,

$$\mathrm{e}^{\mathrm{i}kz} = \sum_{\ell=0}^{\infty}(2\ell+1)\mathrm{i}^\ell j_\ell(kr)P_\ell(\cos\theta), \tag{11}$$

one finds the asymptotic form $\psi_\mathrm{s}(r,\theta) \to r^{-1}\mathrm{e}^{\mathrm{i}kr}f(\theta)$, with the scattering amplitude $f(\theta)$ given in (5).

We now superpose the fields resulting from the counter-propagating plane waves $\mathrm{e}^{\mathrm{i}k(z-b)}$ and $\mathrm{e}^{-\mathrm{i}k(z-b)}$, which, in the absence of the scatterer, would give the stationary (fringing) field $\psi_\mathrm{total} = 2\cos k(z-b)$. We keep the scatterer fixed at the origin. The wave propagating in the $+z$ direction carries the phase factor $\mathrm{e}^{-\mathrm{i}kb}$, so its contribution to the scattered wave does also. The wave propagating in the $-z$ direction has the phase factor $\mathrm{e}^{\mathrm{i}kb}$, and its scattering angle is $\pi-\theta$. Thus the total scattered wave is

$$\psi_\mathrm{s}^\mathrm{total} = \mathrm{e}^{-\mathrm{i}kb}\psi_\mathrm{s}(r,\theta) + \mathrm{e}^{\mathrm{i}kb}\psi_\mathrm{s}(r,\pi-\theta) \to r^{-1}\mathrm{e}^{\mathrm{i}kr}f(\theta) \tag{12}$$

where now the scattering amplitude $f(\theta)$ results from the coherent superposition of the two scattered waves, with their phase factors. It is

$$f(\theta) = k^{-1}\sum_{\ell=0}^{\infty}(2\ell+1)\mathrm{e}^{\mathrm{i}\delta_\ell}\sin\delta_\ell P_\ell(\cos\theta)[\mathrm{e}^{-\mathrm{i}kb} + (-)^\ell\mathrm{e}^{\mathrm{i}kb}] \tag{13}$$

where we have used $P_\ell(-C) = (-)^\ell P_\ell(C)$.

The force on a scatterer is *not* given by substituting the new $f(\theta)$ into (7): the momentum transfer along $+z$ produced by scattering the $\mathrm{e}^{\mathrm{i}k(z-b)}$ wave through θ is $\hbar k(1-\cos\theta)$, while the momentum transfer along $+z$ produced by scattering the $\mathrm{e}^{-\mathrm{i}k(z-b)}$ wave through $\pi-\theta$ is $-\hbar k(1-\cos(\pi-\theta)) = -\hbar k(1+\cos\theta)$, the total momentum z-component transferred to the scatterer being $-2\hbar k\cos\theta$. The effective momentum transfer cross-section is thus

$$\tilde\sigma = -4\pi\int_0^\pi \mathrm{d}\theta\sin\theta\cos\theta|f(\theta)|^2 \tag{14}$$

where $f(\theta)$ is given by (13). We have

$$|f(\theta)|^2 = k^{-2}\sum_\ell\sum_{\ell'}(2\ell+1)(2\ell'+1) \times \sin\delta_\ell\sin\delta_{\ell'}g_\ell^* g_{\ell'}P_\ell(\cos\theta)P_{\ell'}(\cos\theta) \tag{15}$$

where

$$g_\ell \equiv \mathrm{e}^{\mathrm{i}\delta_\ell}[\mathrm{e}^{-\mathrm{i}kb} + (-)^\ell\mathrm{e}^{\mathrm{i}kb}]. \tag{16}$$

The second equality in (8) reduces the double sum in $\tilde\sigma$ to

$$\tilde\sigma = -\frac{8\pi}{k^2}\sum_{\ell=0}^{\infty}(\ell+1)\sin\delta_\ell\sin\delta_{\ell+1}(g_\ell^* g_{\ell+1} + g_{\ell+1}^* g_\ell). \tag{17}$$

Now

$$g_\ell^* g_{\ell+1} + g_{\ell+1}^* g_\ell = 4(-)^{\ell+1}\sin(\delta_\ell - \delta_{\ell+1})\sin 2kb \tag{18}$$

so

$$\tilde\sigma = \sin 2kb\left(\frac{32\pi}{k^2}\right)\sum_{\ell=0}^{\infty}(\ell+1)(-)^\ell \times \sin\delta_\ell\sin\delta_{\ell+1}\sin(\delta_\ell - \delta_{\ell+1}). \tag{19}$$

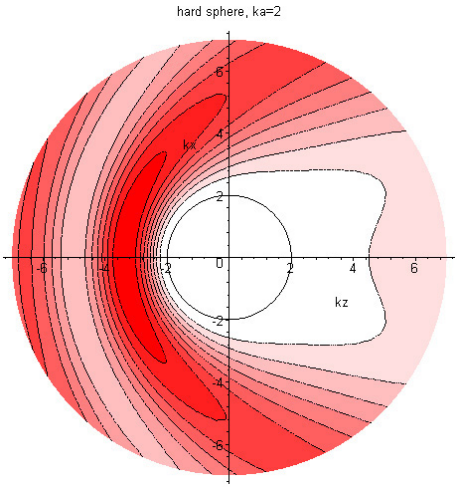

Figure 1. Contours of $|\psi|^2$ for the near field of a hard sphere ($ka = 2$), illuminated from the left. The upstream maximum location follows from approximating the incident plus reflected waves along the negative z axis as $e^{ikz} + re^{-ikz}$, with the reflection amplitude $r = -e^{-2ika}$, to make this total wavefunction zero at $z = -a$. Thus on the negative z axis $\psi \approx 2ie^{-ika} \sin k(z + a)$, with maximum intensity at $k(z + a) \approx -\pi/2$, etc. The first maximum is at $k|z| \approx ka + \pi/2$ which is approximately 3.57 for the case illustrated.

The force on the scatterer in the coherent counter-propagating beams is thus given by a force factor times $\sin 2kb$,

$$\text{force} = 2Ne\tilde{\sigma} \equiv 2NeA \sin 2kb, \tag{20}$$

where A represents an effective area (which can be negative) for the transfer of momentum to the scatterer in the counter-propagating beams,

$$A = \frac{32\pi}{k^2} \sum_{\ell=0}^{\infty} (\ell + 1)(-)^{\ell} \sin \delta_{\ell} \sin \delta_{\ell+1} \sin(\delta_{\ell} - \delta_{\ell+1}). \tag{21}$$

4. An example: force on an impenetrable sphere

Figures 1 and 2 show the value of $|\psi|^2$ near a hard sphere, for which the phase shifts are given by (6), for the unidirectional and counter-propagating beam cases. When the scatterer is small compared to the wavelength $\lambda = 2\pi/k$ (i.e. when $ka \ll 1$), the phase shifts decrease rapidly with ℓ: $\delta_{\ell} \sim (ka)^{2\ell+1}$ [5]. The leading terms, arising from $\delta_0 \approx -ka$ and $\delta_1 \approx -(ka)^3/3$, give

$$\frac{A}{\pi a^2} \approx \frac{-32}{3}(ka)^3. \tag{22}$$

This is small, and negative. The effective potential U of equation (2) is, from (20),

$$U = -k^{-1} 2NeA \cos^2 kb. \tag{23}$$

Thus an impenetrable sphere with radius small compared to the fringe spacing will have effective potential proportional to $+\cos^2 kb$, and will be in stable equilibrium at the potential minima where $\cos kb = 0$, i.e. at the null planes of the fringes, as expected.

As the sphere size is increased, the position of stable equilibrium does not remain at the position of negative interference, however. From (6) we have

$$\sin \delta_{\ell} = \frac{j_{\ell}}{m_{\ell}}, \qquad \cos \delta_{\ell} = \frac{n_{\ell}}{m_{\ell}} \qquad (m_{\ell}^2 \equiv j_{\ell}^2 + n_{\ell}^2) \tag{24}$$

(argument ka is understood), and

$$\sin \delta_{\ell} \sin \delta_{\ell+1} \sin(\delta_{\ell} - \delta_{\ell+1}) = -(ka)^{-2} \frac{j_{\ell} j_{\ell+1}}{m_{\ell}^2 m_{\ell+1}^2} \tag{25}$$

where we have used $j_{\ell} n_{\ell+1} - n_{\ell} j_{\ell+1} = -(ka)^{-2}$. Thus, for hard spheres,

$$\frac{A}{\pi a^2} = -\frac{32}{(ka)^4} \sum_{\ell=0}^{\infty} (\ell + 1)(-)^{\ell} \frac{j_{\ell} j_{\ell+1}}{m_{\ell}^2 m_{\ell+1}^2}. \tag{26}$$

The net force on the sphere is (for a given value of $\sin 2kb$) proportional to A, which is plotted in figure 3. We see that there are alternating negative and positive regions. Up to $ka \approx 2.445$ the sphere prefers to sit at planes of negative interference, but from $ka \approx 2.445$ to 3.985 it prefers to be centred at the positions of maximum intensity, and so on. At the crossover points ($ka \approx 2.445, 3.985, \ldots$) there is zero force on the sphere, everywhere.

When the sphere is large compared to the wavelength ($ka \gg 1$) the spherical Bessel functions take their asymptotic values

$$\begin{aligned} j_{\ell}(ka) &\to (ka)^{-1} \cos(ka - (\ell + 1)\pi/2) \\ n_{\ell}(ka) &\to (ka)^{-1} \sin(ka - (\ell + 1)\pi/2) \end{aligned} \tag{27}$$

up to ℓ of order ka, and then the $j_{\ell}(ka)$ rapidly fall to zero. Thus, for $\ell \lesssim ka$ we have

$$\frac{j_{\ell} j_{\ell+1}}{m_{\ell}^2 m_{\ell+1}^2} \to \frac{1}{2}(ka)^2 (-)^{\ell+1} \sin 2ka \tag{28}$$

and the effective area for the transfer of momentum in counter-propagating beams takes the asymptotic value

$$A \to \frac{32\pi a^2}{(ka)^4} \frac{1}{2}(ka)^2 \sin 2ka \sum_{\ell=0}^{ka} (\ell + 1) \approx 8\pi a^2 \sin 2ka. \tag{29}$$

Thus, at fixed frequency and with sphere size increasing, the effective sphere area oscillates with increasing amplitude. The ratio $A/\pi a^2$ oscillates, with fixed amplitude.

5. Force on a dielectric sphere in an electromagnetic beam

The solution of a problem of scattering of electromagnetic waves by a sphere is usually associated with the names of Mie [7] and Debye [8]. However, as Logan [9] and Kerker [10] point out in their historical notes, several earlier authors also deserve credit, notably Clebsch (in 1863) and Lorenz (in 1890). The theory is treated in several texts [11–14]. We shall follow the notation of van de Hulst [12] with minor changes, the main one being that the time dependence of the complex fields is taken to be $e^{-i\omega t}$ instead of $e^{i\omega t}$, so that the incident plane wave is $e^{i(kz-\omega t)}$, for example. The key results are given in the appendix.

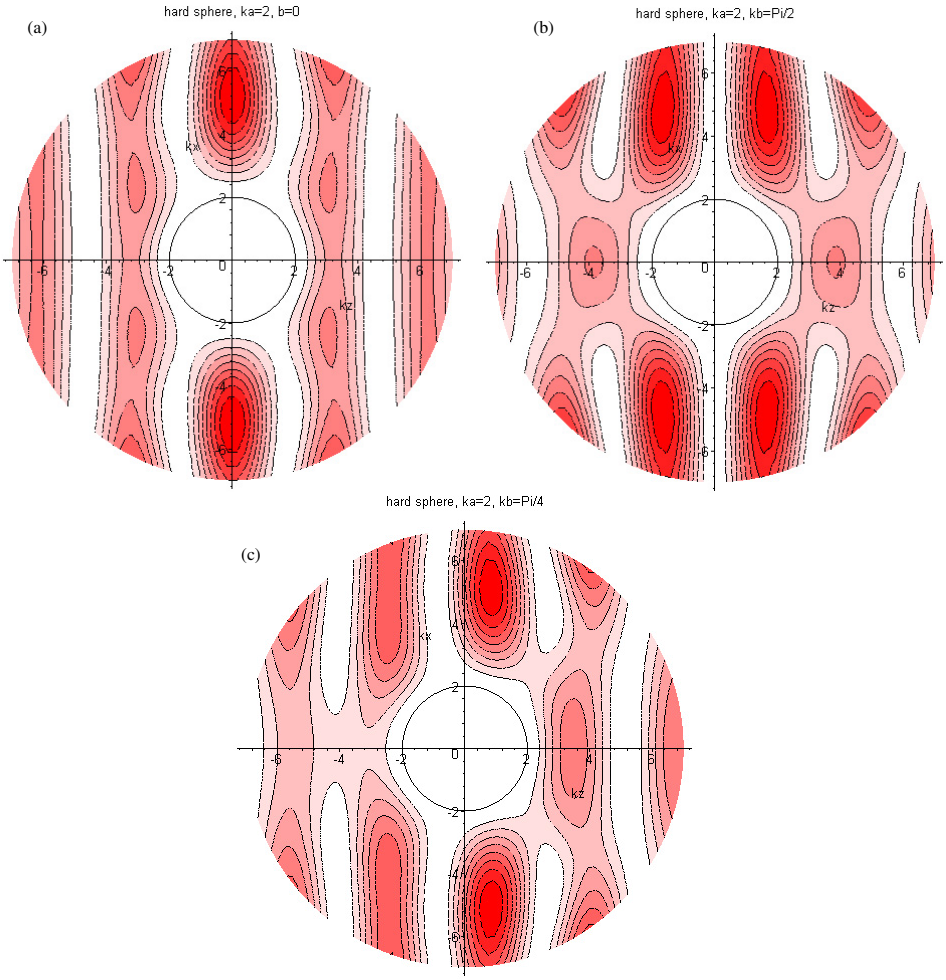

Figure 2. All three figures show contours of $|\psi|^2$ for an impenetrable sphere in the stationary field of two counter-propagating beams $e^{ik(z-b)} + e^{-ik(z-b)} = 2\cos k(z-b)$. The sphere size relative to the wavelength is the same as in figure 1, $a = \lambda/\pi$. The sphere remains at the origin; the fringes shift as b changes. In (a) b is zero, so the sphere is located at what would be a maximum intensity position in its absence. In (b) $kb = \pi/2$, so the sphere sits halfway between intensity maxima. In (c) the sphere is at a position of maximum force: $kb = \pi/4$ and $\sin 2kb$ is unity.

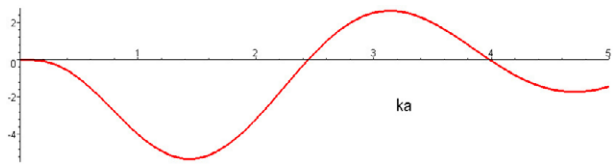

Figure 3. $A/\pi a^2$ for a hard sphere, calculated from (26). Negative A corresponds to a force in the direction of negative z, if $\sin 2kb > 0$. Thus the negative value corresponding to $ka = 2$ implies that the force on the sphere in figure 2(c) is to the left.

For a plane electromagnetic incident wave propagating in the $+z$ direction and polarized in the x direction, the transverse components of the scattered wave are, in the far field ($kr \gg 1$),

$$\begin{aligned} E_\theta = B_\phi &= \frac{1}{ikr} e^{i(kr-\omega t)} \cos\phi S_2(\theta) \\ -E_\phi = B_\theta &= \frac{1}{ikr} e^{i(kr-\omega t)} \sin\phi S_1(\theta) \end{aligned} \tag{30}$$

where S_1 and S_2 are sums over the usual exterior wave complex coefficients a_ℓ and b_ℓ:

$$\begin{aligned} S_1 &= \sum_{\ell=1}^{\infty} \frac{2\ell+1}{\ell(\ell+1)} \{a_\ell \pi_\ell + b_\ell \tau_\ell\}, \\ S_2 &= \sum_{\ell=1}^{\infty} \frac{2\ell+1}{\ell(\ell+1)} \{a_\ell \tau_\ell + b_\ell \pi_\ell\}. \end{aligned} \tag{31}$$

The functions π_ℓ and τ_ℓ are given by (with $\cos\theta = C$ as before)

$$\pi_\ell(C) = \frac{dP_\ell}{dC}, \qquad \tau_\ell(C) = C\pi_\ell - (1-C^2)\frac{d\pi_\ell}{dC}. \tag{32}$$

Equivalent expressions, not containing derivatives, are

$$\pi_\ell = \frac{\ell+1}{1-C^2}(CP_\ell - P_{\ell+1}), \qquad \tau_\ell = \ell(\ell+1)P_\ell - C\pi_\ell. \tag{33}$$

Thus π_ℓ and τ_ℓ may be generated directly from $P_0 = 1$, $P_1 = C$, and the recurrence relation

$$(2\ell+1)CP_\ell = (\ell+1)P_{\ell+1} + \ell P_{\ell-1}. \tag{34}$$

The time-averaged radial component of the Poynting vector is

$$\frac{1}{2(kr)^2}\{\sin^2\phi|S_1|^2+\cos^2\phi|S_2|^2\}. \tag{35}$$

From this one obtains, operating with $\int r^2\,\mathrm{d}\Omega = r^2\int_0^\pi \mathrm{d}\theta\sin\theta\int_0^{2\pi}\mathrm{d}\phi$, the total scattering cross-section σ_s, and $\langle\cos\theta\rangle\sigma_\mathrm{s}$:

$$\sigma_\mathrm{s}=\frac{\pi}{k^2}\int_{-1}^{1}\mathrm{d}C(|S_1|^2+|S_2|^2) \tag{36}$$

$$\langle\cos\theta\rangle\sigma_\mathrm{s}\equiv\frac{\pi}{k^2}\int_{-1}^{1}\mathrm{d}C\,C(|S_1|^2+|S_2|^2). \tag{37}$$

The integrations over θ reduce the double sums to single sums: one finds [8]

$$\sigma_\mathrm{s}=\frac{2\pi}{k^2}\sum_{\ell=1}^{\infty}(2\ell+1)\{|a_\ell|^2+|b_\ell|^2\} \tag{38}$$

$$\langle\cos\theta\rangle\sigma_\mathrm{s}=\frac{4\pi}{k^2}\sum_{\ell=1}^{\infty}\left\{\frac{\ell(\ell+2)}{\ell+1}\,\mathrm{Re}(a_\ell^*a_{\ell+1}+b_\ell^*b_{\ell+1})+\frac{2\ell+1}{\ell(\ell+1)}\,\mathrm{Re}(a_\ell^*b_\ell)\right\}. \tag{39}$$

The extinction cross-section is the sum of the scattering and absorption cross-sections, $\sigma_e=\sigma_\mathrm{s}+\sigma_\mathrm{a}$, and is given by (see [12] (section 9.32))

$$\sigma_e=\frac{2\pi}{k^2}\sum_{\ell=1}^{\infty}(2\ell+1)\,\mathrm{Im}(a_\ell+b_\ell). \tag{40}$$

The cross-section for radiation pressure (arising from the transfer of momentum) is $\sigma_p=\sigma_e-\langle\cos\theta\rangle\sigma_\mathrm{s}$; in the case of non-absorbing scatterers which is being considered here this becomes

$$\sigma_p=[1-\langle\cos\theta\rangle]\sigma_\mathrm{s}, \tag{41}$$

i.e. it is given by the difference between (38) and (39). When the scatterer is in a beam with N quanta per unit volume, each of energy e and momentum e/c, and each travelling at speed c, the force on the scatterer is the rate of momentum transfer, namely

$$\text{force}=Nc\sigma_p e/c=Ne\sigma_p. \tag{42}$$

We have written this down in parallel with the derivation of (10) for the force on a scatterer in a particle beam. The more usual expression is in terms of the magnitude of the Poynting vector, S_0, which gives the energy flux density (energy per unit area per unit time). In terms of N and e, $S_0=Nec$, and so (42) is equivalent to [8, 12, 14]

$$\text{force}=\sigma_p S_0/c. \tag{43}$$

6. Force on a dielectric sphere in counter-propagating beams

We now consider the momentum transfer when a dielectric sphere is in counter-propagating electromagnetic beams, proportional to $\mathrm{e}^{\mathrm{i}k(z-b)}$ and $\mathrm{e}^{-\mathrm{i}k(z-b)}$ respectively (adding to $2\cos k(z-b)$ before interaction with the scatterer). When the wave propagating along $+z$ scatters through angles θ and ϕ, the wave propagating along $-z$ has to scatter through $\pi-\theta$ and $-\phi$ to go in the same direction. The scalar functions u and v all have partial waves with angular dependence as follows (see (A.4)–(A.6)):

$$u_\ell(\theta,\phi)\sim-\sin\theta\cos\phi\pi_\ell(\cos\theta),\qquad v_\ell(\theta,\phi)\sim\sin\theta\sin\phi\pi_\ell(\cos\theta). \tag{44}$$

From $P_\ell(-\cos\theta)=(-)^\ell P_\ell(\cos\theta)$ and (32) or (33) we see that

$$\pi_\ell(-\cos\theta)=(-)^{\ell+1}\pi_\ell(\cos\theta),\qquad \tau_\ell(-\cos\theta)=(-)^\ell\tau_\ell(\cos\theta). \tag{45}$$

Thus

$$u_\ell(\pi-\theta,-\phi)=(-)^{\ell+1}u_\ell(\theta,\phi),\qquad v_\ell(\pi-\theta,-\phi)=(-)^\ell v_\ell(\theta,\phi). \tag{46}$$

The $\mathrm{e}^{\mathrm{i}k(z-b)}$ and $\mathrm{e}^{-\mathrm{i}k(z-b)}$ plane waves carry phase factors $\mathrm{e}^{-\mathrm{i}\beta}$ and $\mathrm{e}^{\mathrm{i}\beta}(\beta=kb)$ relative to the scatterer placed at the origin. Thus the total partial waves due to both beams have the form

$$[\mathrm{e}^{-\mathrm{i}\beta}+(-)^{\ell+1}\mathrm{e}^{\mathrm{i}\beta}]u_\ell(\theta,\phi)\equiv m_\ell(\beta)u_\ell(\theta,\phi)\qquad [\mathrm{e}^{-\mathrm{i}\beta}+(-)^\ell\mathrm{e}^{\mathrm{i}\beta}]v_\ell(\theta,\phi)\equiv p_\ell(\beta)v_\ell(\theta,\phi). \tag{47}$$

In the case of the scattered partial waves, the scattering coefficients are a_ℓ and b_ℓ for $\mathrm{e}^{\mathrm{i}kz}$ incident. For $\mathrm{e}^{\mathrm{i}k(z-b)}$ and $\mathrm{e}^{-\mathrm{i}k(z-b)}$ incident the coefficients become $a_\ell m_\ell$ and $b_\ell p_\ell$. The transverse components of the fields in the scattered wave, when $kr\gg1$, take the form (30), with S_1 and S_2 replaced by

$$T_1=\sum_{\ell=1}^{\infty}\frac{2\ell+1}{\ell(\ell+1)}\{a_\ell m_\ell\pi_\ell+b_\ell p_\ell\tau_\ell\},\qquad T_2=\sum_{\ell=1}^{\infty}\frac{2\ell+1}{\ell(\ell+1)}\{a_\ell m_\ell\tau_\ell+b_\ell p_\ell\pi_\ell\}. \tag{48}$$

The momentum transfer from the field to the scatterer per quantum carrying momentum e/c is $(-2\cos\theta)e/c$, in parallel with section 3, so the momentum transfer effective 'cross-section', which may again be negative, is (cf (37) and (41))

$$\tilde\sigma_p=-\frac{2\pi}{k^2}\int_{-1}^{1}\mathrm{d}C\,C\{|T_1|^2+|T_2|^2\}. \tag{49}$$

In the integral in (49) two types of term will appear:

$$\int_{-1}^{1}\mathrm{d}C\,C(\pi_\ell\pi_{\ell'}+\tau_\ell\tau_{\ell'})=\frac{2\ell^2(\ell+1)(\ell+2)^2}{(2\ell+1)(2\ell+3)}\delta_{\ell',\ell+1}+\frac{2(\ell-1)^2\ell(\ell+1)^2}{(2\ell-1)(2\ell+1)}\delta_{\ell',\ell-1} \tag{50}$$

$$\int_{-1}^{1}\mathrm{d}C\,C\pi_\ell\tau_{\ell'}=\frac{\ell(\ell+1)}{2\ell+1}\delta_{\ell',\ell}. \tag{51}$$

(These integrals were evaluated by Debye [8] in his consideration of the radiation force on a dielectric sphere: they were needed in the derivation of (39).) Thus (49) will contain the following terms:

$$p_\ell^*p_{\ell\pm1}=-2\mathrm{i}(-)^\ell\sin2\beta=p_\ell^*m_\ell\qquad m_\ell^*m_{\ell\pm1}=2\mathrm{i}(-)^\ell\sin2\beta. \tag{52}$$

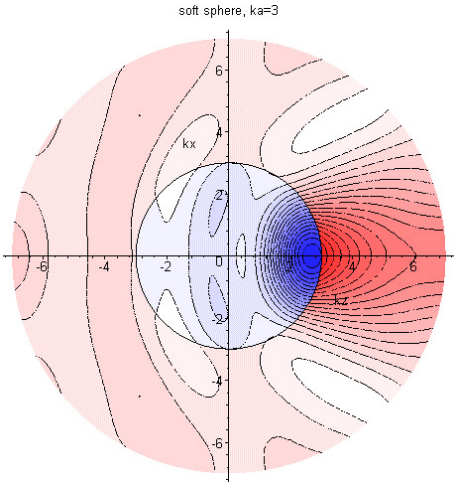

Figure 4. Contours of $|\psi|^2$ for the near field around an attractive square well, when a plane wave is incident from the left. The depth of the well is chosen to correspond to a relative refractive index of 1.2. The sphere diameter is of the same order as the wavelength ($ka = 3$, $2a = 3\lambda/\pi$), so ray optics does not correctly locate the hot-spot, as noted in the text.

Let $A_\ell = \frac{2\ell+1}{\ell(\ell+1)} a_\ell m_\ell$, $B_\ell = \frac{2\ell+1}{\ell(\ell+1)} b_\ell p_\ell$. Then

$$\begin{aligned}|T_1|^2 + |T_2|^2 &= \sum_\ell \sum_{\ell'} \{(A_\ell^* \pi_\ell + B_\ell^* \tau_\ell)(A_{\ell'} \pi_{\ell'} + B_{\ell'} \tau_{\ell'}) \\ &\quad + (A_\ell^* \tau_\ell + B_\ell^* \pi_\ell)(A_{\ell'} \tau_{\ell'} + B_{\ell'} \pi_{\ell'})\} \\ &= \sum_\ell \sum_{\ell'} \{(A_\ell^* A_{\ell'} + B_\ell^* B_{\ell'})(\pi_\ell \pi_{\ell'} + \tau_\ell \tau_{\ell'}) \\ &\quad + (A_\ell^* B_{\ell'} + B_\ell^* A_{\ell'} + B_\ell A_{\ell'}^* + A_\ell B_{\ell'}^*) \pi_\ell \tau_{\ell'}\}. \end{aligned} \tag{53}$$

Use of (50)–(52) gives, after some reduction,

$$\tilde{\sigma}_p = \frac{16\pi}{k^2} \sin 2\beta \sum_{\ell=1}^{\infty} (-)^\ell \times \operatorname{Im}\left\{ \frac{\ell(\ell+2)}{\ell+1} (a_\ell^* a_{\ell+1} + b_\ell^* b_{\ell+1}) + \frac{2\ell+1}{\ell(\ell+1)} a_\ell^* b_\ell \right\}. \tag{54}$$

Note the similarity with Debye's formula for $\langle \cos\theta \rangle \sigma_s$, equation (39). The net force on the dielectric sphere thus contains the $\sin 2kb$ factor:

$$\text{force} = \tilde{\sigma}_p S_0/c \equiv (A S_0/c) \sin 2kb \tag{55}$$

where A (which can be negative) is the effective area for the transfer of momentum to the scatterer:

$$A = \frac{16\pi}{k^2} \sum_{\ell=1}^{\infty} (-)^\ell \operatorname{Im}\left\{ \frac{\ell(\ell+2)}{\ell+1} (a_\ell^* a_{\ell+1} + b_\ell^* b_{\ell+1}) + \frac{2\ell+1}{\ell(\ell+1)} a_\ell^* b_\ell \right\}. \tag{56}$$

The effective potential for the sphere in the fringing field is, from (1), (2), and (55),

$$U = -\frac{A S_0}{kc} \cos^2 kb. \tag{57}$$

When A is greater than zero, the preferred position for the sphere is centred on the fringe maxima.

These results will be illustrated in section 8 for dielectric spheres which are of similar size to the wavelength, but first we shall look at the case of sphere size small compared to the wavelength.

7. Long wavelength limit (Rayleigh scattering)

We consider non-absorbing spheres with real dielectric constant ε. To order $(ka)^6$ the non-zero coefficients are

$$\begin{aligned} a_1 &= \frac{2}{3}\frac{\varepsilon-1}{\varepsilon+2}(ka)^3 + \frac{2}{5}\frac{(\varepsilon-1)(\varepsilon-2)}{(\varepsilon+2)^2}(ka)^5 \\ &\quad + \mathrm{i}\frac{4}{9}\frac{(\varepsilon-1)^2}{(\varepsilon+2)^2}(ka)^6 + \mathrm{O}(ka)^7 \\ b_1 &= \tfrac{1}{45}(\varepsilon-1)(ka)^5 + \mathrm{O}(ka)^7 \\ a_2 &= \frac{1}{15}\frac{\varepsilon-1}{(2\varepsilon+3)}(ka)^5 + \mathrm{O}(ka)^7. \end{aligned} \tag{58}$$

The scattering cross-section in a unidirectional beam is therefore, from (38),

$$\sigma_s = 2\pi a^2 \left[\frac{4}{3} \left(\frac{\varepsilon-1}{\varepsilon+2} \right)^2 (ka)^4 + \mathrm{O}(ka)^6 \right]. \tag{59}$$

The leading term in $\langle \cos\theta \rangle \sigma_s$, given in (39), contains $\mathrm{Re}(a_1^* a_2)$ and $\mathrm{Re}(a_1^* b_1)$, both of order $(ka)^8$. Thus we regain the well-known result (see for example [12] (section 6.3))

$$\sigma_p = [1 - \langle \cos\theta \rangle]\sigma_s = \frac{8\pi}{3} a^2 \left[\left(\frac{\varepsilon-1}{\varepsilon+2} \right)^2 (ka)^4 + \mathrm{O}(ka)^6 \right]. \tag{60}$$

The force is $\sigma_p S_0/c$.

The force on a non-absorbing sphere in counter-propagating beams is $(A S_0/c) \sin 2kb$, where A is given by (56). The leading term in A when ε is real is of order $(ka)^9$, namely

$$\frac{64}{135}\pi a^2 \frac{(\varepsilon-1)^3}{(\varepsilon+2)^2} \frac{\varepsilon+3}{2\varepsilon+3} (ka)^9. \tag{61}$$

Nonabsorbing particles which are small compared to the wavelength accordingly experience a force smaller by a factor of order $(ka)^5$ in a counter-propagating beam, compared to the force in a unidirectional beam. The corresponding ratio in quantum particle beams is of order $(ka)^3$. Since A is positive for small particles with $\varepsilon > 1$, and the effective potential in the fringes is given by (57), we see that small dielectric spheres will sit at fringe intensity maxima. (Small bubbles in a fluid will be in stable equilibrium at intensity minima.)

8. Comparison of the quantum and electromagnetic scattering in a particular case

The Mellor–Bain experiment [1] uses the evanescent wave of an infrared Nd:YAG laser beam ($\lambda = 1064$ nm in vacuum), retro-reflected to provide the pair of counter-propagating beams. The evanescent waves are in water, with constructive interference fringes spaced $\lambda/2n_{\text{water}} \approx 400$ nm apart when the angle of incidence is close to the critical angle. The spheres are silica, with refractive index 1.60, so the relative silica/water refractive index is $1.60/1.33 \approx 1.20$. The relative dielectric constant ε is the square of this. The wavelength is shorter inside the spheres; the corresponding quantum potential is therefore an attractive square well, with depth V_0 such as to make $1 + V_0/e = \varepsilon$, where $e = \hbar^2 k^2/2m$ is the energy of a particle in the beam (see for example section 1–3, equation (46), of [15]).

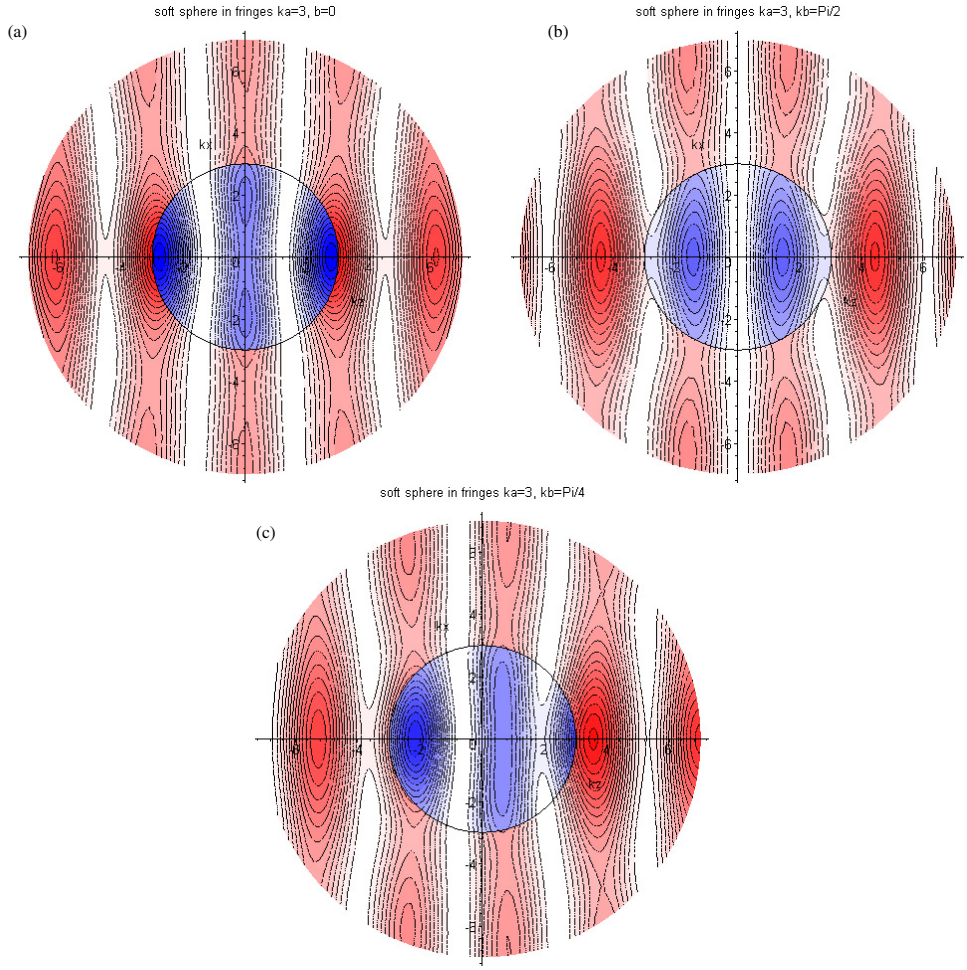

Figure 5. Contours of $|\psi|^2$ for a soft sphere (parameters as in figure 4) in counter-propagating beams. (a) The sphere is centred on a constructive interference fringe maximum. (b) As for (a), but now the soft sphere is centred on an interference minimum. The force on it is zero by symmetry, as it is in (a). (c) The spherical square well is now centred halfway between an interference maximum and an interference minimum of the unperturbed counter-propagating beams. This is the position of maximum force. According to figure 6(a) the force is to the left (the effective area A is negative at $ka = 3$).

We expect some correspondence between plots of $|\psi|^2$ in the quantum case, and of $|E|^2$ in the electromagnetic case, for the same value of ka, since both are built up from solutions of the same Helmholtz equation. The sphere diameters used in the experiment range from 0.3 to 1.0 μm. The wavelength of the evanescent waves in the water, when incidence is close to critical, is 0.8 μm. Thus ka ranges from 1.2 to 3.9, approximately. We shall use $ka = 3$ (wavelength $= (\pi/3)$ diameter) as a representative value, with ka large enough to display the diffraction hot-spots in the near field.

Figure 4 shows $|\psi|^2$ for the near field around a square well with depth 0.44 times the energy (to correspond to a relative refractive index n_r of 1.2), in a unidirectional beam, incident from the left. Note that the intensity maximum ('hot-spot') *cannot* be explained by geometric optics, which predicts a focus (for paraxial rays) at

$$z_m = a\frac{n_r}{2(n_r - 1)}. \tag{62}$$

When the relative refractive index n_r is 1.2, the distance z_m from the sphere centre is $3a$ according to (62), and ray optics predicts a hot-spot at $kz_m = 9$ in figure 4, whereas it occurs at $kz_m \approx 2.68$, inside the sphere. The value of $|\psi|^2$ at maximum is 4.37 times the value of $|\psi|^2$ far from the sphere, at $ka = 3$. (For $ka = 4$ we find a maximum intensity at $kz_m \approx 3.77, 6.68$ times the ambient value.)

Figures 5 show the near field around the same sphere ($ka = 3$), now in counter-propagating beams. The constructive interference fringes are centred respectively on the sphere, symmetrically on either side of the sphere, and halfway between these zero-force configurations. The net force on the sphere at any position relative to the fringes is given by (20) and (21), with the phase shifts δ_ℓ appropriate to scattering by an attractive square well, namely (see for example [5] (equations (19.15) and (19.26)))

$$\tan\delta_\ell = \frac{\gamma_\ell j_\ell(ka) - j'_\ell(ka)}{\gamma_\ell n_\ell(ka) - n'_\ell(ka)}, \qquad \gamma_\ell = \frac{q}{k}\frac{j'_\ell(qa)}{j_\ell(qa)}. \tag{63}$$

In (63) a prime indicates a derivative with respect to the argument, and q is the wavenumber inside the well, $q = n_r k$ ($n_r = 1.2$ in the figure). Figure 6(a) shows $A/\pi a^2$, where A is the effective area in the force expression (20).

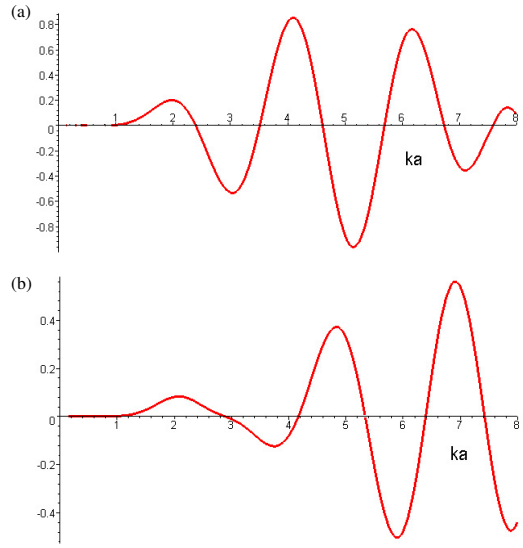

Figure 6. (a) $A/\pi a^2$ for an attractive square well, $V_0/e = 0.44$ (refractive index 1.20 relative to the ambient medium), versus ka. (b) $A/\pi a^2$ for a dielectric sphere of relative refractive index 1.20.

In figure 6(b) we show $A/\pi a^2$ for the dielectric sphere, for which A is given by (56) and the force is given by (55). The curves for the quantum and electromagnetic cases are qualitatively similar in the location of their leading zeros; the first three occur at $ka \approx 2.38$ and 2.87, 3.52 and 4.16, 4.60 and 5.33, respectively. However, it is clear that one cannot rely on the scalar theory for quantitative prediction of the electromagnetic force.

Finally, figures 7 and 8 give the distribution of the magnitude of the electric energy density, proportional to $|E|^2$, for a dielectric sphere ($ka = 3, n_r = 1.2$), respectively in a unidirectional beam, and centred on a fringe maximum, a fringe minimum, and at the position of maximum force. The incident plane electromagnetic waves are polarized in the x direction. There is accordingly an azimuthal dependence in the electric and magnetic fields, but the variation of $|E|^2$ with azimuthal angle ϕ is not strong: in figure 7 we show two plots, one at $\phi = 0$ in the $y = 0$ plane and one at $\phi = \pi/2$ in the $x = 0$ plane. The figures relating to fringes are all drawn for the $y = 0$ plane, i.e. in the plane of polarization.

9. Radiation force on a dielectric sphere in a liquid

Our result (55) for the force on a dielectric sphere applies to a sphere in vacuum. Its physical basis is Newton's law: force equals the rate of change of momentum. We calculated the rate at which the electromagnetic momentum is being changed by scattering off the sphere, assuming that the momentum of a quantum of energy e is e/c, or equivalently that the momentum density of the field is the energy flux density (Poynting vector) divided by c^2. (It has been shown that *localized* wavepackets obeying Maxwell's equations always have momentum smaller than energy$/c$ [16], but here we have plane waves incident, and we use the asymptotic forms of the scattered waves—that is, highly delocalized states.)

How should our force equations be modified to apply to the experimental case, where the dielectric spheres are in a liquid? One aspect is clear: in calculating the electromagnetic scattering coefficients a_ℓ and b_ℓ, we should use (and have already used, in our example of section 8) the relative refractive index $n_r = n_s/n_a$, where n_s and n_a are the refractive indices of the dielectric sphere and of the ambient medium (water, in the Mellor–Bain experiment). When $n_s = n_a$ the sphere becomes optically invisible, and there is no scattering and no force; the coefficients a_ℓ and b_ℓ all go to zero when $n_r \to 1$, linearly in $n_r - 1$.

But what should one put for the momentum of the light in the liquid? There are two main contenders for the momentum associated with a packet of energy e in a medium of refractive index n_a,

$$p_A = \frac{1}{n_a}\frac{e}{c}, \qquad p_M = n_a\frac{e}{c} \tag{64}$$

associated with Abraham and Minkowski, respectively. The Abraham–Minkowski controversy is nearly a century old, and still active [17–22]. The experiments of Jones and Richards [17] established that the force on a mirror submerged in various liquids is proportional to the refractive index of the liquid (other factors being equal) to $\pm 1.2\%$. Later experiments of Jones and Leslie [18] confirmed that 'electromagnetic momentum is proportional to the refractive index, to $\pm 0.05\%$'. Gordon [19] has noted that 'radiation' pressure is actually a combination of the force exerted directly by the field within the object and that exerted on the object by mechanical pressures induced in the ambient medium by the field. A review of the experimental situation to 1979 is given by Brevik [20]. The effective momenta of photons in dielectrics are considered by Loudon [21], who finds the 'force enhanced by the refractive index of the transparent medium'. We adopt the view that [22] 'while Abraham's expression is indeed the momentum of the field, the measured momentum also includes the matter contribution, and its value coincides with Minkowski's result'. The implication for the problem at hand is that (55) becomes

$$\text{force} = n_a(AS_0/c)\sin 2kb \tag{65}$$

where the effective area A of (56) is to contain coefficients a_ℓ and b_ℓ calculated with the relative refractive index $n_r = n_s/n_a$, with wavenumber k equal to n_a times the vacuum wavenumber.

10. Discussion

We have considered the forces on spheres in counter-propagating coherent beams. In both the quantum particle and electromagnetic cases we found a simple form for the force, proportional to $\sin 2kb$. (This is simpler than the form $\sum_{m=1}^{\infty} A_m \sin 2mkb$ demanded by the periodicity of the interference fringes.) The force is determined by the same phase shifts δ_ℓ and vector wave coefficients a_ℓ and b_ℓ which arise in computing the scattering cross-sections.

An interesting aspect of the results is that the multiplier A of $\sin 2kb$ is an oscillatory function of ka, so there exist sphere sizes (relative to the wavelength of the radiation) for which the force on the sphere is zero, whatever its position within the fringing field.

If the sphere radius and the refractive indices of the sphere and ambient medium are known, no adjustable parameters remain in the force expression. Thus the radiation forces can

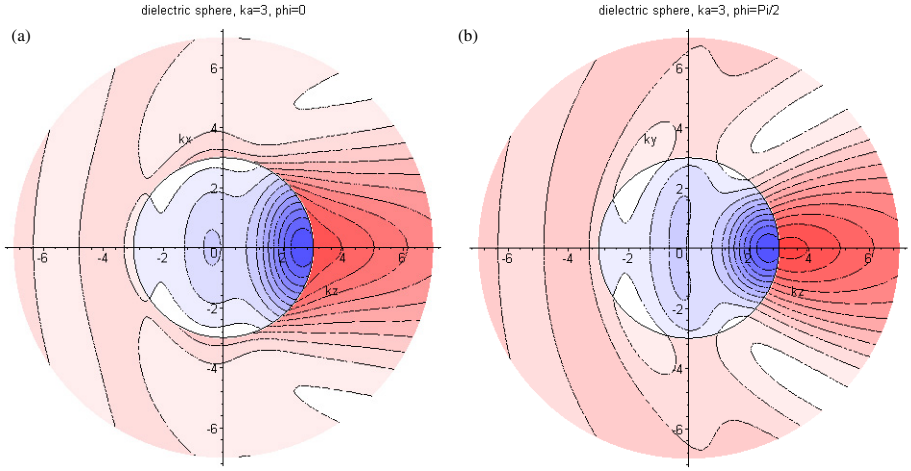

Figure 7. Contours of $|\mathbf{E}|^2$ for a dielectric sphere in a unidirectional beam polarized along the x direction. In (a) we show the electric energy density in the plane $y = 0$ ($\sin\phi = 0$). Part (b) is for the $x = 0$ plane ($\cos\phi = 0$); in this plane the radial component of $\mathbf{E}$ is zero, and $|\mathbf{E}|^2$ is continuous at the sphere surface.

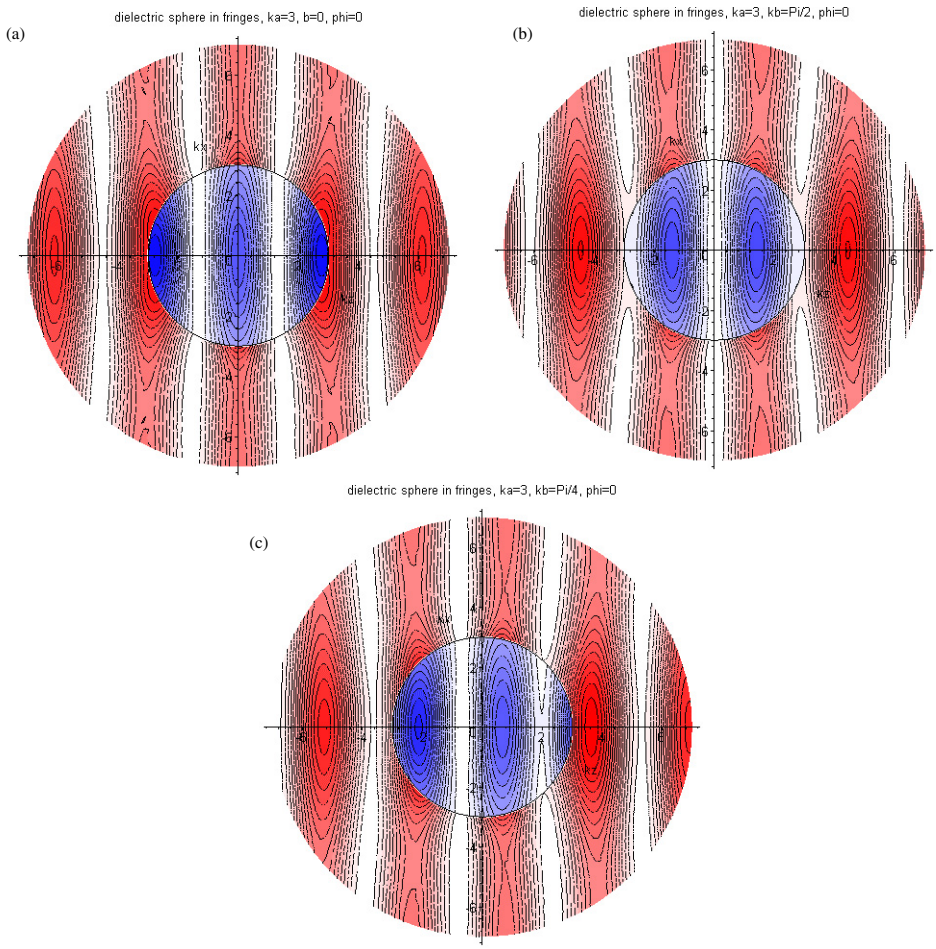

Figure 8. (a) Contours of $|\mathbf{E}|^2$ for the dielectric sphere of figure 7, centred on the position of an interference maximum of the unperturbed counter-propagating beams. The plot is in the plane of polarization of the incident beams. (b) As for (a), with the sphere centred on an interference minimum. Note that $|\mathbf{E}|^2$ is in general not continuous at the sphere surface, since only the tangential components of $\mathbf{E}$ are continuous at the surface. (c) The same dielectric sphere, at a position of maximum force. From figure 6(b) we see that A is negative at $ka = 3$, so the force is to the left (the equilibrium position for this ka value is at interference minima).

be calculated exactly, and can then be used as a gauge for other forces that act on the dielectric spheres. However, the results of this paper are, in the case of evanescent waves, restricted to the immediate neighbourhood of the critical angle, since we have assumed the counter-propagating beams to be homogeneous plane waves.

A further complication arises when highly focused beams are used. In this case the fringes will be of finite (and varying) width, narrowest in the focal region. The theory of optical tweezers for unidirectional focused beams is available [23], and can in principle be generalized to counter-propagating beams by using the methods developed here.

Acknowledgments

It is a pleasure to thank Colin Bain and Chris Mellor for stimulating discussions about their experiment, and Tim Softley and the Warden and Fellows of Merton College, Oxford, for their warm hospitality during Michaelmas Term of 2004.

Appendix. Scattering by a dielectric sphere

We summarize the standard results [7–14] to provide definitions of the fields and scattering coefficients. The notation parallels that of van de Hulst [12]. Details of proofs are omitted.

If ψ satisfies the Helmholtz equation $(\nabla^2 + q^2)\,\psi = 0$, so do the vectors $\mathbf{M} = \nabla \times \mathbf{r}\psi$, $\mathbf{N} = q^{-1}\nabla \times \mathbf{M}$. Also $q\mathbf{M} = \nabla \times \mathbf{N}$. Let $q = nk = n\omega/c$, n being the refractive index. The Maxwell equations for harmonic waves with $\mathrm{e}^{-\mathrm{i}\omega t}$ time dependence, $\nabla \times \mathbf{E} = \mathrm{i}k\mathbf{B}$ and $\nabla \times \mathbf{B} = -\mathrm{i}kn^2\mathbf{E}$, are satisfied by

$$\mathbf{E} = \mathbf{M}_v + \mathrm{i}\mathbf{N}_u, \qquad \mathbf{B} = n(\mathbf{M}_u - \mathrm{i}\mathbf{N}_v) \tag{A.1}$$

when u and v satisfy $(\nabla^2 + q^2)\psi = 0$, and $\mathbf{M}_u = \nabla \times \mathbf{r}u$, etc.

For a linearly polarized incident plane wave $\mathrm{e}^{\mathrm{i}kz}$ (the time factor $\mathrm{e}^{-\mathrm{i}\omega t}$ is omitted here and below), with $\mathbf{E}^0 = \hat{\mathbf{x}}\mathrm{e}^{\mathrm{i}kz}$, $\mathbf{B}^0 = \hat{\mathbf{y}}\mathrm{e}^{\mathrm{i}kz}$, the field components along $\hat{\mathbf{r}}$, $\hat{\boldsymbol{\theta}}$, and $\hat{\boldsymbol{\varphi}}$ are

$$\begin{aligned} E^0_{\mathrm{r}} &= \sin\theta\cos\phi\mathrm{e}^{\mathrm{i}kz} & B^0_{\mathrm{r}} &= \sin\theta\sin\phi\mathrm{e}^{\mathrm{i}kz} \\ E^0_{\theta} &= \cos\theta\cos\phi\mathrm{e}^{\mathrm{i}kz} & B^0_{\theta} &= \cos\theta\sin\phi\mathrm{e}^{\mathrm{i}kz} \\ E^0_{\phi} &= -\sin\phi\mathrm{e}^{\mathrm{i}kz} & B^0_{\phi} &= \cos\phi\mathrm{e}^{\mathrm{i}kz}. \end{aligned} \tag{A.2}$$

The components of $\mathbf{M} = \nabla \times \mathbf{r}\psi$ and $q\mathbf{N} = \nabla \times \mathbf{M}$, based on a solution of $(\nabla^2 + q^2)\psi = 0$, are

$$\begin{aligned} M_{\mathrm{r}} &= 0 & qN_{\mathrm{r}} &= (\partial^2_{\mathrm{r}} + q^2)(r\psi) \\ M_{\theta} &= \frac{1}{r\sin\theta}\partial_{\phi}(r\psi) & qN_{\theta} &= \frac{1}{r}\partial_{\mathrm{r}}\partial_{\theta}(r\psi) \\ M_{\phi} &= -\frac{1}{r}\partial_{\theta}(r\psi) & qN_{\phi} &= \frac{1}{r\sin\theta}\partial_{\mathrm{r}}\partial_{\phi}(r\psi). \end{aligned} \tag{A.3}$$

The incident field components (A.2) are given by (A.1) with $n = 1 (q = k)$ and

$$\begin{aligned} u_0 &= -\sin\theta\cos\phi\sum_{\ell=1}^{\infty}\frac{2\ell+1}{\ell(\ell+1)}\mathrm{i}^{\ell}j_{\ell}(kr)\pi_{\ell}(\cos\theta) \\ v_0 &= \sin\theta\sin\phi\sum_{\ell=1}^{\infty}\frac{2\ell+1}{\ell(\ell+1)}\mathrm{i}^{\ell}j_{\ell}(kr)\pi_{\ell}(\cos\theta) \end{aligned} \tag{A.4}$$

(some properties of $\pi_\ell(C) = \mathrm{d}P_\ell(C)/\mathrm{d}C$ were given in section 5). The corresponding functions for the scattered wave are spherically diverging waves at large kr. We write them as

$$\begin{aligned} u_{\mathrm{s}} &= -\sin\theta\cos\phi\sum_{\ell=1}^{\infty}a_{\ell}\frac{2\ell+1}{\ell(\ell+1)}\mathrm{i}^{\ell}\mathrm{i}h^{(1)}_{\ell}(kr)\pi_{\ell}(\cos\theta) \\ v_{\mathrm{s}} &= \sin\theta\sin\phi\sum_{\ell=1}^{\infty}b_{\ell}\frac{2\ell+1}{\ell(\ell+1)}\mathrm{i}^{\ell}\mathrm{i}h^{(1)}_{\ell}(kr)\pi_{\ell}(\cos\theta). \end{aligned} \tag{A.5}$$

The solutions in the interior of the sphere are

$$\begin{aligned} u_i &= -\sin\theta\cos\phi\sum_{\ell=1}^{\infty}c_{\ell}\frac{2\ell+1}{\ell(\ell+1)}\mathrm{i}^{\ell}j_{\ell}(qr)\pi_{\ell}(\cos\theta) \\ v_i &= \sin\theta\sin\phi\sum_{\ell=1}^{\infty}d_{\ell}\frac{2\ell+1}{\ell(\ell+1)}\mathrm{i}^{\ell}j_{\ell}(qr)\pi_{\ell}(\cos\theta). \end{aligned} \tag{A.6}$$

The continuity of the tangential components of $\mathbf{E}$ and $\mathbf{B}$ at $r = a$ implies the continuity of rv, nru, $\partial_{\mathrm{r}}(rv)$ and $n^{-1}\partial_{\mathrm{r}}(ru)$. Since derivatives of ru and rv are involved, it is convenient to work with the functions

$$\begin{gathered} S_\ell(kr) = krj_\ell(kr), \qquad C_\ell(kr) = -krn_\ell(kr), \\ Z_\ell = C_\ell + \mathrm{i}S_\ell. \end{gathered} \tag{A.7}$$

Continuity of nru and $n^{-1}\partial_{\mathrm{r}}(ru)$ gives, with $x = ka$, $y = qa$,

$$\begin{gathered} S_\ell(x) + a_\ell Z_\ell(x) = nc_\ell S_\ell(y) \\ k(S'_\ell(x) + a_\ell Z'_\ell(x)) = n^{-1}qc_\ell S'_\ell(y). \end{gathered} \tag{A.8}$$

Continuity of rv and $\partial_{\mathrm{r}}(rv)$ gives

$$\begin{gathered} S_\ell(x) + b_\ell Z_\ell(x) = d_\ell S_\ell(y) \\ k(S'_\ell(x) + b_\ell Z'_\ell(x)) = qd_\ell S'_\ell(y). \end{gathered} \tag{A.9}$$

This set of equations is solved by (note that $Z_\ell(x)S'_\ell(x) - S_\ell(x)Z'_\ell(x) = C_\ell(x)S'_\ell(x) - S_\ell(x)C'_\ell(x) = 1$)

$$\begin{aligned} a_\ell &= -\frac{S_\ell(x)S'_\ell(y) - nS'_\ell(x)S_\ell(y)}{Z_\ell(x)S'_\ell(y) - nZ'_\ell(x)S_\ell(y)}, \\ b_\ell &= -\frac{S'_\ell(x)S_\ell(y) - nS_\ell(x)S'_\ell(y)}{Z'_\ell(x)S_\ell(y) - nZ_\ell(x)S'_\ell(y)} \\ c_\ell &= \frac{-1}{Z_\ell(x)S'_\ell(y) - nZ'_\ell(x)S_\ell(y)}, \\ d_\ell &= \frac{-1}{Z'_\ell(x)S_\ell(y) - nZ_\ell(x)S'_\ell(y)}. \end{aligned} \tag{A.10}$$

When the refractive index is real (no absorption) the scattering coefficients a_ℓ and b_ℓ can be written in terms of real phase shifts α_ℓ and β_ℓ:

$$a_\ell = \mathrm{e}^{\mathrm{i}\alpha_\ell}\sin\alpha_\ell, \qquad \text{where}$$
$$\tan\alpha_\ell = -\frac{S(x)S'(y) - nS'(x)S(y)}{C(x)S'(y) - nC'(x)S(y)} \tag{A.11}$$

$$b_\ell = \mathrm{e}^{\mathrm{i}\beta_\ell}\sin\beta_\ell, \qquad \text{where}$$
$$\tan\beta_\ell = -\frac{S'_\ell(x)S_\ell(y) - nS_\ell(x)S'_\ell(y)}{C'_\ell(x)S_\ell(y) - nC_\ell(x)S'_\ell(y)}. \tag{A.12}$$

An alternative way of writing (A.11) and (A.12) is

$$a_\ell = \frac{\tan\alpha_\ell}{1 - \mathrm{i}\tan\alpha_\ell}, \qquad b_\ell = \frac{\tan\beta_\ell}{1 - \mathrm{i}\tan\beta_\ell}. \tag{A.13}$$

As ka increases the coefficients a_ℓ and b_ℓ move anticlockwise around a circle of unit diameter, centred on $\mathrm{i}/2$ in the complex plane. The coefficients a_ℓ and b_ℓ defined here are i times the corresponding van de Hulst coefficients. This makes no difference in the evaluation of cross-sections, or of any other physical quantity. The advantage of the present definitions is that all coefficients are real to lowest order in ka when the refractive index n is real: all begin as $n^2 - 1$ times a power of ka times a positive number (see for example (58)).

When kr is large, we see from (27) that

$$h_\ell^{(1)}(kr) \to \frac{\mathrm{e}^{\mathrm{i}kr}}{\mathrm{i}kr}(-\mathrm{i})^\ell \tag{A.14}$$

so the u_s and v_s of (A.5) take the asymptotic values

$$\begin{aligned} u_\mathrm{s} &\to -\sin\theta\cos\phi\frac{\mathrm{e}^{\mathrm{i}kr}}{\mathrm{i}kr}\sum_{\ell=1}^{\infty}\frac{2\ell+1}{\ell(\ell+1)}a_\ell\pi_\ell(\cos\theta) \\ v_\mathrm{s} &\to \sin\theta\sin\phi\frac{\mathrm{e}^{\mathrm{i}kr}}{\mathrm{i}kr}\sum_{\ell=1}^{\infty}\frac{2\ell+1}{\ell(\ell+1)}b_\ell\pi_\ell(\cos\theta). \end{aligned} \tag{A.15}$$

The far field values of the transverse components of the scattered fields, given in (30), follow from (A.3) and (A.15) with the use of (32).

References

[1] Mellor C and Bain C D 2005 at press

[2] Kawata S and Sugiura T 1992 Movement of micrometer-sized particles in the evanescent field of a laser beam *Opt. Lett.* **17** 772–4

[3] Almass E and Brevik I 1995 Radiation forces on a micrometer-sized sphere in an evanescent field *J. Opt. Soc. Am.* B **12** 2429–38

[4] Lester M and Nieto-Vesperinas M 1999 Optical forces on microparticles in an evanescent laser field *Opt. Lett.* **24** 936–8

[5] Schiff L I 1968 *Quantum Mechanics* 3rd edn (New York: McGraw-Hill)

[6] Bates D R 1962 *Atomic and Molecular Processes* (New York: Academic Press) p 645

[7] Mie G 1908 Beiträge zur optik trüber medien, speziell kolloidaler Metallösungen *Ann. Phys., Lpz.* **25** 377–445

[8] Debye P 1909 Der Lichtdruck auf Kugeln von beliebigen material *Ann. Phys., Lpz.* **30** 57–136

[9] Logan N A 1965 Survey of some early studies of the scattering of plane waves by a sphere *Proc. IEEE* **53** 773–85

[10] Kerker M 1969 *The Scattering of Light and Other Electromagnetic Radiation* (New York: Academic) section 3.4

[11] Stratton J A 1941 *Electromagnetic Theory* (New York: McGraw-Hill)

[12] van de Hulst H C 1957 *Light Scattering by Small Particles* (New York: Wiley)

[13] Born M and Wolf E 1959 *Principles of Optics* (Cambridge: Cambridge University Press)

[14] Bohren C F and Huffman D R 1983 *Absorption and Scattering of Light by Small Particles* (New York: Wiley)

[15] Lekner J 1987 *Theory of Reflection of Electromagnetic and Particle Waves* (Dordrecht: Nijhoff/Kluwer)

[16] Lekner J 2004 Energy and momentum of electromagnetic pulses *J. Opt. A: Pure Appl. Opt.* **6** 146–7

[17] Jones R V and Richards J C S 1954 The pressure of radiation in a refracting medium *Proc. R. Soc.* A **221** 480–98

[18] Jones R V and Leslie B 1978 The measurement of optical radiation pressure in dispersive media *Proc. R. Soc.* A **360** 347–63

[19] Gordon J P 1973 Radiation forces and momenta in dielectric media *Phys. Rev.* A **8** 14–21

[20] Brevik I 1979 Experiments in phenomenological electrodynamics and the electromagnetic energy–momentum tensor *Phys. Rep.* **52** 133–201

[21] Loudon R 2002 Theory of the radiation pressure on dielectric surfaces *J. Mod. Opt.* **49** 821–38

[22] Feigel A 2004 Quantum vacuum contribution to the momentum of dielectric media *Phys. Rev. Lett.* **92** 020404, 1–4

[23] Maia Neto P A and Nussenzveig H M 2000 Theory of optical tweezers *Europhys. Lett.* **50** 702–8